ACS Pharmacology & Translational Science

pubs.acs.org/ptsci

Article

Validation and Invalidation of SARS-CoV-2 Papain-like Protease Inhibitors

Chunlong Ma and Jun Wang*

Cite This: ACS Pharmacol. Transl. Sci. 2022, 5, 102−109

Read Online

ACCESS | Metrics & More | Article Recommendations

ABSTRACT: SARS-CoV-2 encodes two viral cysteine proteases, the main protease (M^{pro}) and the papain-like protease (PL^{pro}), both of which are validated antiviral drug targets. PL^{pro} is involved in the cleavage of viral polyproteins as well as immune modulation by removing ubiquitin and interferon-stimulated gene product 15 (ISG15) from host proteins. Therefore, targeting PL^{pro} might be a two-pronged approach. Several compounds including YM155, cryptotanshinone, tanshinone I, dihydrotanshinone I, tanshinone IIA, SJB2-043, 6-thioguanine, and 6-mercaptopurine were recently identified as SARS-CoV-2 PL^{pro} inhibitors through high-throughput screenings. In this study, we aim to validate/invalidate the reported PL^{pro} inhibitors using a combination of PL^{pro} target-specific assays including enzymatic FRET assay, thermal shift binding assay (TSA), and cell-based FlipGFP assay. Collectively, our results showed that all compounds tested either did not show binding or led to denaturation of PL^{pro} in the TSA binding assay, which might explain their weak enzymatic inhibition in the FRET assay. In addition, none of the compounds showed cellular PL^{pro} inhibition as revealed by the FlipGFP assay. Therefore, more efforts are needed to search for potent and specific SARS-CoV-2 PL^{pro} inhibitors.

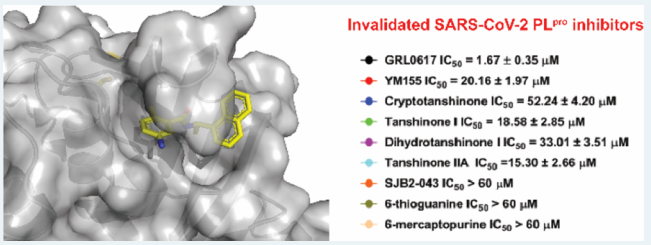

KEYWORDS: *SARS-CoV-2, papain-like protease, GRL0617, FlipGFP, antiviral*

The COVID-19 pandemic is a timely reminder for the urgent need of antivirals, especially broad-spectrum antivirals that could be used as the first-line defense against not only the current pandemic but also future pandemics.[1] SARS-CoV-2, SARS-CoV, and MERS-CoV are the three coronaviruses in the β-coronavirus family that caused pandemics/epidemics in humans.[2] SARS-CoV and MERS-CoV had higher mortality rates than SARS-CoV-2.[3] However, SARS-CoV-2 has a much higher transmission rate than SARS-CoV and MERS-CoV, which leads to far greater infection cases and death tolls.

SARS-CoV-2 shares 86% sequence identity with SARS-CoV, which renders the rapid understanding of its viral pathogenicity feasible. SARS-CoV-2 expresses two viral proteases during the viral replication, the main protease (M^{pro}; nsp5) and the papain-like protease (PL^{pro}; nsp3). Both are cysteine proteases and have been validated as antiviral drug targets.[4−6] PL^{pro} and M^{pro} cleave the viral polyproteins pp1a and pp1ab at 3 and more than 11 sites, respectively, resulting in individual functional viral proteins for the assembly of a viral replication complex. Compared to PL^{pro}, M^{pro} is a more amenable drug target and has been the central focus of COVID-19 antiviral discovery. Structurally disparate compounds have been reported as M^{pro} inhibitors from either drug repurposing screening or rational design.[7,8] Although a large number of reported M^{pro} inhibitors were later proven to be promiscuous cysteine modifiers,[9−13] several M^{pro} inhibitors have been validated as specific inhibitors and have shown *in vivo* antiviral efficacy in animal model studies.[14−18] Significantly, two Pfizer M^{pro} inhibitors PF-07304814 and PF-07321332 are advanced to human clinical trials.[17,18]

PL^{pro} is the second viral cysteine protease that cleaves the viral polypeptide at three different sites during viral replication. In addition, PL^{pro} modulates host immune response by cleaving ubiquitin and ISG15 (interferon-induced gene 15) from host proteins.[19−21] In contrast to M^{pro} inhibitors, the development of PL^{pro} inhibitors is still at its infancy.[22] The most promising PL^{pro} inhibitors are the naphthalene-based GRL0617 series of compounds (Figure 1A).[6,21,23−25] However, their antiviral potency and pharmacokinetic properties need to be further optimized for the *in vivo* animal model study. PL^{pro} specifically recognizes the P4-P1 sequence Leu-X-Gly-Gly that is conserved among the nsp1/2, nsp2/3, and nsp3/4 cleavage sites at the viral polyprotein.[26] The featureless P1 and P2 binding pockets present a grand challenge in developing potent PL^{pro} inhibitors.[26] As the drug-binding site

Received: November 3, 2021
Published: January 24, 2022

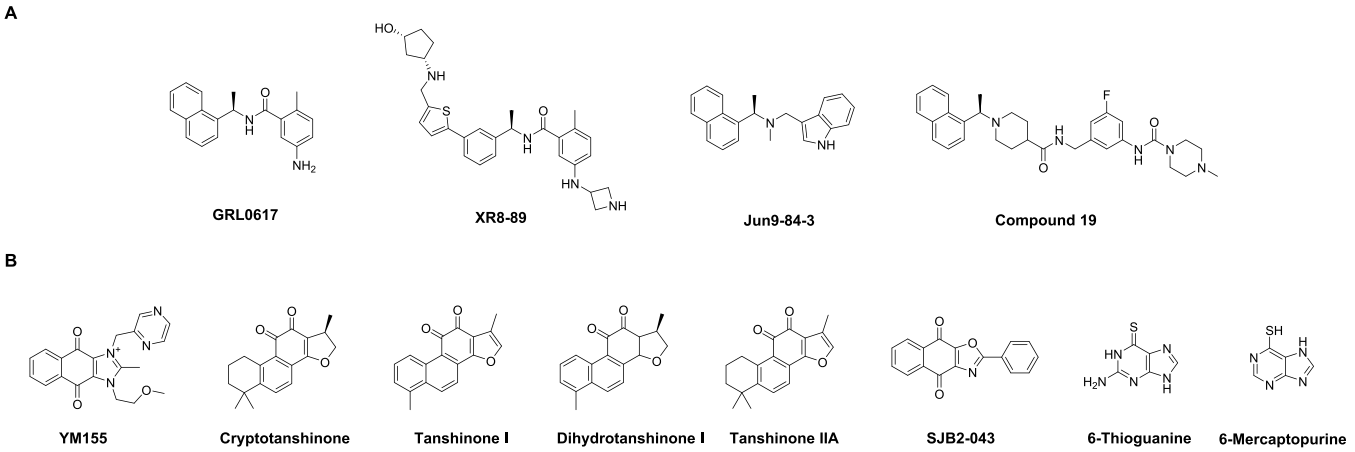

Figure 1. SARS-CoV-2 PL^{pro} inhibitors. (A) GRL0617 analogs. (B) Structurally disparate PL^{pro} inhibitors identified from high-throughput screening or drug repurposing screening of bioactive compounds.

is far away from the catalytic cysteine 111 (>10 Å), the majority of the reported PL^{pro} inhibitors are noncovalent inhibitors.[7] Although peptidomimetic covalent PL^{pro} inhibitors have been reported, no antiviral activity is shown.[26] To identify additional novel PL^{pro} inhibitors, several high-throughput screenings have been performed and structurally disparate compounds are found to inhibit PL^{pro} (Figure 1B).[27−30] It is intriguing that structurally diverse compounds can act on the same protein; we therefore are interested in validating/invalidating the reported PL^{pro} inhibitors using a combination of orthogonal assays including the activity-based FRET enzymatic assay, the thermal shift binding (TSA) assay, and the cell-based FlipGFP assay. The purpose is to prioritize well-characterized PL^{pro} inhibitors for medicinal chemistry optimization. The FRET assay is the gold standard assay for protease, which measures the activity of the purified enzyme in the presence of a compound. However, the FRET assay results might be complicated by the fluorescence interference compound, alkylating reagent, or redox compound. The TSA assay is a binding assay that measures the direct binding between the small molecule and the protein. High-affinity binders generally stabilize the protein, leading to the increase in the melting temperature. The cell-based FlipGFP assay measures the cellular protease activity and can rule out compounds that are cytotoxic, membrane-impermeable, or lack the cellular target engagement due to off-target effects. Collectively, in contrast to the literature-reported results, our data showed that the examined non-GRL0617-based PL^{pro} inhibitors (Figure 1B) had weak enzymatic inhibition and no cellular PL^{pro} inhibition; therefore, they should not be referenced as specific PL^{pro} inhibitors.

RESULTS

Through a high-throughput screening of over 6,000 bioactive compounds using a quenched fluorescent substrate RLRGG-AMC, Zhao *et al.* identified four compounds, YM155, cryptotanshinone, tanshinone I, and GRL0617, as potent PL^{pro} inhibitors with IC_{50} values from 1.39 to 5.63 μM.[29] In the plaque reduction assay, YM155, cryptotanshinone, and tanshinone l inhibited SARS-CoV-2 replication in Vero E6 cells with EC_{50} values of 0.17, 0.70, and 2.26 μM, respectively. The X-ray crystal structure of SARS-CoV-2 PL^{pro} with YM155 was solved (PDB: 7D7L), revealing three different binding sites that are located in the thumb domain, the zinc-finger motif, and the substrate-binding pocket. In the substrate binding pocket, YM155 induces a conformational change of Y268 on the BL2 loop and forms a π-stacking interaction, which is similar to the binding mode of GRL0617. Binding at the thumb domain likely impedes the interaction between PL^{pro} and ISG15. The third binding site at the zinc-finger domain might perturb its stability; however, this mechanism remains to be validated.

In our validation study, the positive control GRL0617 showed similar enzymatic inhibition with an IC_{50} of 1.67 μM (Figure 2A). However, we found that the enzymatic inhibition potency for YM155, cryptotanshinone, and tanshinone I against PL^{pro} was ∼10-fold less active than previously reported and the IC_{50} values from our study were 20.16, 52.24, and 18.58 μM, respectively (Figure 2A and Table 1). The discrepancy might be caused by the different substrates used. In Zhao *et al.*'s study, RLRGG-AMC was used, while we used a FRET substrate Dabcyl-FTLRGG/APTKV-Edans, which spans both the P and P′ sites. Nevertheless, in the thermal shift binding assay, YM155 had no effect on the stability of PL^{pro}, while cryptotanshinone and tanshinone I caused destabilization of the protein (Figure 2B and Table 1). In the cell-based FlipGFP assay,[6] the result for YM155 was not conclusive as it was cytotoxic to the 293T cells (Figure 2C). Both cryptotanshinone and tanshinone I were not active (EC_{50} > 60 μM) (Figure 2C). Overall, our results indicate that cryptotanshinone and tanshinone I were not specific PL^{pro} inhibitors, while YM155 might be a specific PL^{pro} inhibitor. However, the large discrepancy between the enzymatic inhibition (IC_{50} = 20.16 μM) and the reported cellular antiviral activity of YM155 (EC_{50} = 0.17 μM) suggests that the other mechanisms might contribute to its potent antiviral activity against SARS-CoV-2.

In another study, cryptotanshinone and two analogs dihydrotanshinone I and tanshinone IIA were identified as SARS-CoV-2 PL^{pro} inhibitors through a high-throughput screening (HTS).[28] Cryptotanshinone, dihydrotanshinone I, and tanshinone IIA inhibited SARS-CoV-2 PL^{pro} with IC_{50} values of 1.336, 0.5861, and 1.571 μM, respectively. It is noted that no complete inhibition was observed for cryptotanshinone; therefore, the IC_{50} value might not be trustworthy. To rule out the possibility of fluorescence interference, these compounds were also tested in the gel-based PL^{pro} assay using the GST-nsp2/3-MBP substrate. All these compounds

https://doi.org/10.1021/acsptsci.1c00240
ACS Pharmacol. Transl. Sci. 2022, 5, 102−109

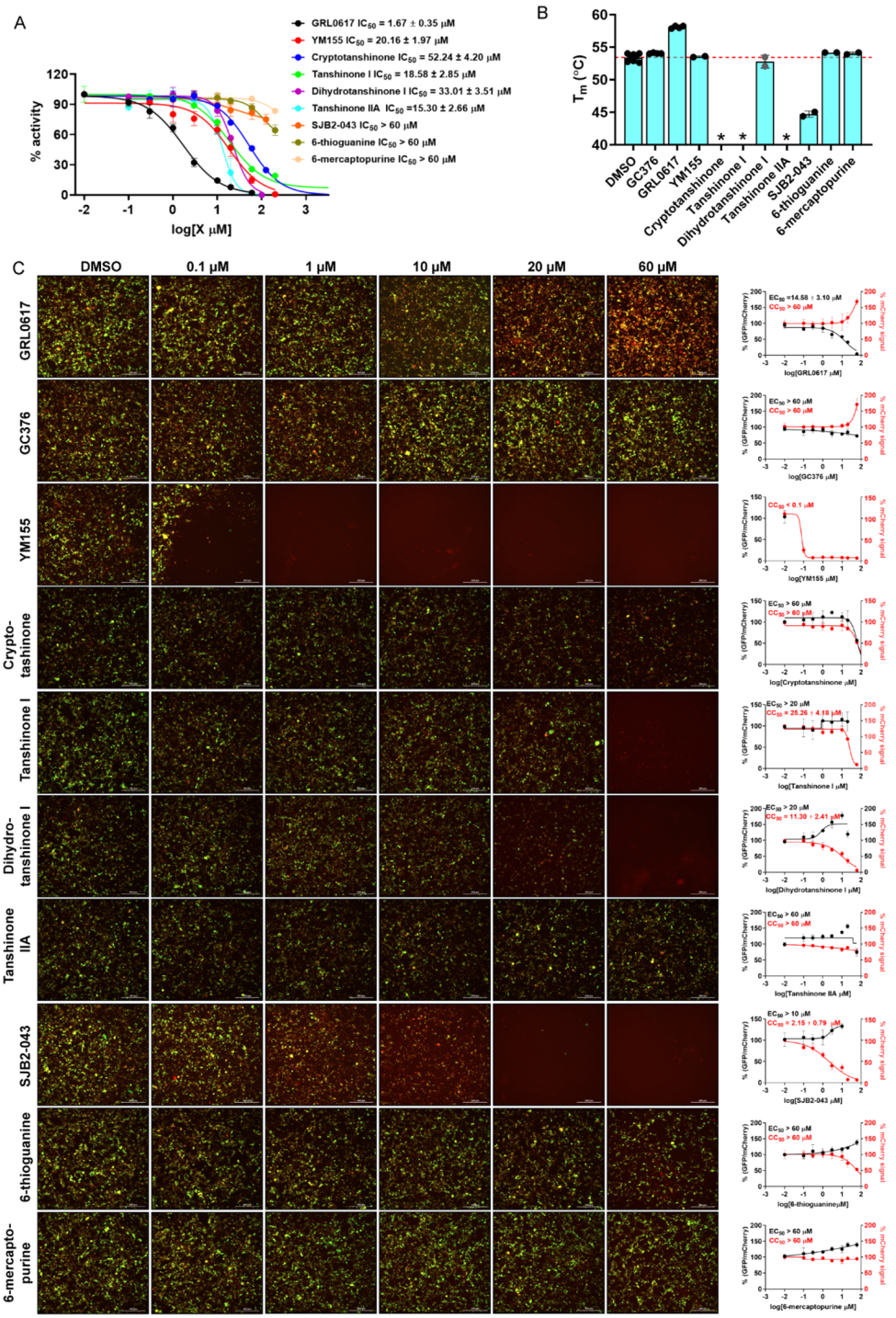

Figure 2. Pharmacological characterization of SARS-CoV-2 PL^{pro} inhibitors. (A) Enzymatic inhibitory activity against SARS-CoV-2 PL^{pro} in the FRET-based assay. (B) Thermal shift assay of the SARS-CoV-2 PL^{pro} inhibitors in stabilizing SARS-CoV-2 PL^{pro}. The asterisk (*) means that the melting peak was not observed in the presence of the inhibitor. The dashed red line indicates the mean of SARS-CoV-2 PL^{pro} T_m in the absence of testing inhibitors. (C) Cell-based FlipGFP assay for the quantification of the cellular activity of SARS-CoV-2 PL^{pro} inhibitors. Representative images of the FlipGFP-PL^{pro} assay with the positive control GRL0617 and the negative control GC-376. Dose−response curves of the ratio of GFP/mCherry fluorescence with SARS-CoV-2 PL^{pro} inhibitors were plotted at right side column; mCherry signal alone was used to normalize the protein expression level or calculate compound cytotoxicity.

inhibited the digestion of the protein substrate with tanshinone IIA and cryptotanshinone showing higher potency than dihydrotanshinone I. Dihydrotanshinone I also inhibited the deubiquitinase and deISGlase activities of PL^{pro} in the gel-based digestion assay. In the SARS-CoV-2 antiviral assay in Vero E6 cells, dihydrotanshinone I had the highest potency with an EC_{50} of 8.148 μM, while cryptotanshinone and tanshinone I were not active (EC_{50} > 200 μM). The lack of correlation between the enzymatic inhibition and the cellular antiviral activity might be due to cell membrane permeability or off-target effects.

https://doi.org/10.1021/acsptsci.1c00240
ACS Pharmacol. Transl. Sci. 2022, 5, 102−109

Table 1. Validation/Invalidation of SARS-CoV-2 PL^{pro} Inhibitors[a]

	Reported Enzymatic inhibition IC_{50} (μM)	Reported Antiviral EC_{50}/CC_{50} (μM)	Validation FRET IC_{50} (μM)	TSA ΔTm (°C)	FlipGFP
GC-376	N. T.	3.37 ± 1.68/>100	> 60	0.62	> 60
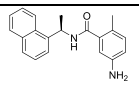 GRL0617	1.39 ± 0.26 1.789 [28]	3.18 ± 0.71/~500 32.64 [28]	1.67 ± 0.35	4.88	14.58 ± 3.10
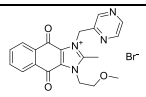 YM155	2.47 ± 0.46 [29]	0.17 ± 0.02/~400 [29]	20.16 ± 1.97	0.11	Toxic
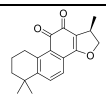 Cryptotanshinone	5.63 ± 1.45 [29] 1.336 [28]	0.70 ± 0.09/>300 [29] >200 [28]	52.24 ± 4.20	No peak	> 60
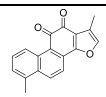 Tanshinone I	2.21 ± 0.10 [29]	2.26 ± 0.11/>200 [29]	18.58 ± 2.85	No peak	> 60
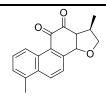 Dihydrotanshinone I	0.5861[28]	8.148 [28]	33.01 ± 3.51	-0.66	> 20
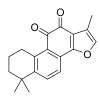 Tanshinone IIA	1.571 [28]	>200 [28]	15.30 ± 2.66	No peak	> 60
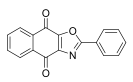 SJB2-043	0.56 ± 0.16 [27]	N.T.	> 60	-8.72	> 10 (toxic)
 6-thioguanine	0.5 (TAP-nsp123) 1.0 (TAP-nap23) 0.1 (de-ISGylation) 72 ± 12 [31]	2.13 ± 1.16/35.5 ± 9.45 (Vero E6)	> 60	0.74	> 60
 6-mercaptopurine	N.T.	N.T.	> 60	0.60	> 60

[a]N.T., not tested.

In our validation study, both dihydrotanshinone I and tanshinone IIA were greater than 10-fold less potent in the enzymatic assay with IC_{50} values of 33.01 and 15.30 μM, respectively (Figure 2A and Table 1). Dihydrotanshinone I did not bind to PL^{pro} as shown by the results from the TSA assay (Figure 2B). Tanshinone IIA led to denaturation of the protein (no melting peak). Dihydrotanshinone I and tanshinone IIA were not active in the FlipGFP assay (IC_{50} > 20 μM) (Figure 2C). Overall, it appears that dihydrotanshinone I and tanshinone IIA were not specific SARS-CoV-2 PL^{pro} inhibitors, and the antiviral activity of dihydrotanshinone I might involve other mechanisms.

Cho *et al.* reported SJB2-043 as a SARS-CoV-2 PL^{pro} inhibitor through a focused screening of a library of deubiquitinase inhibitors.[27] SJB2-043 did not achieve complete inhibition and had an apparent IC_{50} of 0.56 μM. When Ub-AMC was used as a substrate, the IC_{50} of SJB2-043 was 0.091 μM. Similarly, no complete inhibition was achieved. In comparison, the positive control GRL0617 showed complete inhibition when both Z-LRGG-AMC and Ub-AMC were used as substrates, and the IC_{50} values were 1.37 and 1.80 μM, respectively. Molecular docking suggests that SJB2-043 binds to an allosteric site in PL^{pro}.

https://doi.org/10.1021/acsptsci.1c00240
ACS Pharmacol. Transl. Sci. 2022, 5, 102−109

When repeated in our assay, SJB2-043 did not inhibit SARS-CoV-2 PL^{pro} (IC_{50} > 60 μM) (Figure 2A). The discrepancy might be caused by different methods used for data fitting. In our assay, SJB2-043 did not achieve more than 50% inhibition at the highest concentration tested, which is 60 μM; therefore, we deemed the IC_{50} greater than 60 μM. In the TSA binding assay, SJB2-043 led to the destabilization of PL^{pro} (ΔT_m = −8.72 °C) (Figure 2B). The result from the FlipGFP assay was not conclusive as SJB2-043 was cytotoxic (Figure 2C). Overall, SJB2-043 might not be a specific SARS-CoV-2 PL^{pro} inhibitor and only shows partial inhibition.

Swaim *et al.* reported that 6-thioguanine inhibited SARS-CoV-2 replication in Vero E6 cells with an EC_{50} of 2.13 μM.[30] Mechanistic studies showed that 6-thioguanine had potent inhibition against PL^{pro} in cells and *in vitro* using the TAP-nsp123, TAP-nsp23, and Pro-ISG15-HA substrates. Another study from Fu *et al.* showed that 6-thioguanine inhibited SARS-CoV-2 PL^{pro} in the enzymatic assay with an IC_{50} of 72 μM.[31] In our study, 6-thioguanine was not active in the FRET-based enzymatic assay (IC_{50} > 60 μM) (Figure 2A). 6-Thioguanine also did not show binding in the TSA assay nor inhibition in the FlipGFP assay (Figure 2B,C). As such, the antiviral activity of 6-thioguanine might involve other mechanisms. 6-Mercaptopurine, which is an analog of 6-thioguanine, was similarly not active in all three assays (Figure 2 and Table 1). Therefore, it can be concluded that 6-thioguanine and 6-mercaptopurine were not SARS-CoV-2 PL^{pro} inhibitors.

DISCUSSION

Drug repurposing is often viewed as a fast-track drug discovery approach since it can potentially bypass the length safety tests before entering clinical trials.[32] However, we should remain cautiously optimistic about this approach.[33] Since the existing bioactive compounds were not specifically designed and optimized for the screening drug target, the identified hits need to be vigorously characterized to validate the target specificity. SARS-CoV-2 M^{pro} and PL^{pro} are cysteine proteases that are prone to nonspecific inhibition by alkylating agents or redox cycling compounds. Indeed, our recent studies, together with others, have collectively shown that a number of reported M^{pro} inhibitors including ebselen, carmofur, disulfiram, and shikonin are promiscuous nonspecific cysteine protease inhibitors.[9−13] With our continuous interest in the validation/invalidation of literature-reported M^{pro} and PL^{pro} inhibitors, in this study, we characterized eight PL^{pro} inhibitors using a combination of FRET-based enzymatic assay, TSA binding assay, and cell-based FlipGFP-PL^{pro} assay. It is expected that specific inhibitors will show consistent results from all three assays. Among the compounds tested, cryptotanshinone, tanshinone I, dihydrotanshinone I, and tanshinone IIA were also previously reported as potent SARS-CoV PL^{pro} inhibitors with IC_{50} values ranging from 0.8 to 8.8 μM.[34] Interestingly, they also inhibited SARS-CoV M^{pro} with IC_{50} values ranging from 14.4 to 226.7 μM. Since M^{pro} and PL^{pro} do not share structural and sequence similarities, the dual inhibitory activities of these tanshinones, coupled with the weak PL^{pro} enzymatic inhibition from our study, suggest that they might have a promiscuous mechanism of action.

Similarly, 6-thioguanine and 6-mercaptopurine were previously reported as SARS-CoV PL^{pro} inhibitors with IC_{50} values of 5.0 and 21.6 μM, respectively.[35,36] In addition, Cheng *et al.* reported that 6-thioguanine and 6-mercaptopurine are competitive inhibitors of MERS-CoV PL^{pro} with IC_{50} values of 24.4 and 26.9 μM, respectively.[37] In contrast, YM155 and SJB2-043 were not previously shown to inhibit SARS-CoV PL^{pro}. Given the 82.6% sequence similarity between SARS-CoV-2 PL^{pro} and SARS-CoV PL^{pro}, it is not a surprising finding that cryptotanshinone, tanshinone I, dihydrotanshinone I, tanshinone IIA, and 6-thioguanine were also reported as SARS-CoV-2 PL^{pro} inhibitors from recent studies. Nevertheless, our independent study has shown that all eight compounds had drastically reduced enzymatic inhibition against SARS-CoV-2 PL^{pro} compared to reported values (Table 1). In addition, all compounds either had no effect or destabilize PL^{pro} as shown by the TSA binding assay (Table 1). Furthermore, cryptotanshinone, tanshinone I, dihydrotanshinone I, tanshinone IIA, 6-thioguanine, and 6-mercaptopurine were not active in the FlipGFP-PL^{pro} assay, suggesting that there is a lack of cellular PL^{pro} target engagement. YM155 and SJB2-043 were cytotoxic; therefore, it remains unknown whether they can selectively bind to PL^{pro} inside the cell. From the chemical structure perspective, YM155, cryptotanshinone, tanshinone, dihydrotanshinone I, tanshinone IIA, and SJB2-043 are quinones, which are known as cysteine modifiers.[38] Overall, our study calls for more stringent validation of the reported SARS-CoV-2 PL^{pro} inhibitors to avoid the failure in the follow-up lead optimization and translational development.

In addition to the compounds examined (Table 1), ebselen[39] and its analogs,[40] as well as disulfiram,[39,41,42] were also reported as SARS-CoV-2 PL^{pro} inhibitors. Our previous results have shown that both ebselen and disulfiram are promiscuous PL^{pro} inhibitors and their inhibition against PL^{pro} is abolished in the presence of reducing reagent DTT.[10] In addition, ebselen and disulfiram also inhibit several other unrelated cysteine proteases in the absence of DTT, suggesting that both compounds are nonspecific cysteine modifiers.

It is important to highlight that the focus of this study is the pharmacological characterization of reported SARS-CoV-2 PL^{pro} inhibitors. Although our results have shown that cryptotanshinone, tanshinone I, dihydrotanshinone I, tanshinone IIA, and 6-thioguanine are nonspecific PL^{pro} inhibitors, they have been reported to inhibit SARS-CoV-2 replication in cell culture (Table 1). Therefore, our results should not be interpreted as a discouragement to further pursue them as potential SARS-CoV-2 antivirals. If their antiviral activity is validated, follow-up studies are needed to delineate their mechanism of action.

MATERIALS AND METHODS

Chemicals and Peptide Substrate. The SARS-CoV-2 PL^{pro} substrate Dabcyl-FTLRGG/APTKV-Edans was synthesized by the solid-phase synthesis, and the detailed procedure was described in our previous publication.[6] The testing compounds were ordered from the following sources: tanshinone I (Sigma T5330), dihydrotanshinone I (Sigma D0947), tanshinone IIA (Sigma SML2517), cryptotanshinone (Sigma C5624), YM-155 (APExBIO A4221), and SJB2-043 (APExBIO A3823).

SARS-CoV-2 PL^{pro} Expression and Purification. SARS-CoV-2 papain-like protease (PL^{pro}) gene (ORF 1ab 1564−1876) from strain BetaCoV/Wuhan/WIV04/2019 with *Escherichia coli* codon optimization was ordered from GenScript in the pET28b(+) vector. The detailed expression and purification procedures were previously described.[6]

https://doi.org/10.1021/acsptsci.1c00240
ACS Pharmacol. Transl. Sci. 2022, 5, 102−109

FRET-Based Enzymatic Assay. For the IC_{50} measurement with the FRET-based assay, the reaction was carried out in 96-well format with 100 μL of 200 nM PL^{pro} protein in a PL^{pro} reaction buffer (50 mM HEPES (pH 7.5), 5 mM DTT, and 0.01% Triton X-100); 1 μL of testing compounds at various concentrations was added to each well and was incubated at 30 °C for 30 min. The reaction was initiated by adding 1 μL of 1 mM FRET substrate and was monitored in a Cytation 5 image reader with filters for excitation at 360/40 nm and emission at 460/40 nm at 30 °C for 1 h. The initial velocity of the enzymatic reaction was calculated from the initial 10 min enzymatic reaction. The IC_{50} was calculated by plotting the initial velocity against various concentrations of testing compounds by the use of a four-parameter variable slope dose−response curve in Prism 8 software.

Differential Scanning Fluorimetry (DSF). The thermal shift binding assay (TSA) was carried out using a Thermo Fisher QuantStudio 5 Real-Time PCR system as described previously.[6]

Cell-Based FlipGFP-PL^{pro} Assay. The cell-based FlipGFP-PL^{pro} assay was established as previously described. Briefly, 293T cells were maintained in Dulbecco's modified Eagle's medium (DMEM), supplemented with 10% heat-inactivated FBS and 1% penicillin−streptomycin antibiotics in a 37 °C incubator with 5% CO_2. A 96-well Greiner plate (catalog no. 655090) was seeded with 293T cells to overnight 70−90% confluency. Fifty nanograms of pcDNA3-flipGFP-PLpro-T2A-mCherry plasmid and 50 ng of pcDNA3.1-SARS2-PL^{pro} were used for each well in the presence of transfection reagent TransIT-293 (Mirus) per the manufacturer's protocol. Three hours after transfection, 1 μL of testing compound was added to each well at 100-fold dilution. Two days after transfection, images were obtained with a Cytation 5 imaging reader (Biotek) with GFP and mCherry channels. SARS-CoV-2 PL^{pro} protease activity was evaluated by the ratio of GFP signal intensity over the mCherry signal intensity. The compound FlipGFP-PLP assay IC_{50} value was calculated by plotting the GFP/mCherry signal to the testing compound concentration with a four-parameter variable slope dose−response function in Prism 8. The mCherry signal alone was utilized to determine the compound cytotoxicity.

AUTHOR INFORMATION

Corresponding Author

Jun Wang − *Department of Pharmacology and Toxicology, College of Pharmacy, The University of Arizona, Tucson, Arizona 85721, United States;* orcid.org/0000-0002-4845-4621; Phone: 520-626-1366; Email: junwang@pharmacy.arizona.edu; Fax: 520-626-0749

Author

Chunlong Ma − *Department of Pharmacology and Toxicology, College of Pharmacy, The University of Arizona, Tucson, Arizona 85721, United States*

Complete contact information is available at: https://pubs.acs.org/10.1021/acsptsci.1c00240

Author Contributions

C.M. performed the enzymatic assay, thermal shift binding assay, and FlipGFP assay. J.W. designed and supervised this study. J.W. wrote the manuscript with contribution from C.M.

Notes

The authors declare no competing financial interest.

ACKNOWLEDGMENTS

This research was supported by the National Institutes of Health (NIH) (grants AI147325, AI157046, and AI158775) and the Arizona Biomedical Research Centre Young Investigator grant (ADHS18-198859) to J.W.

REFERENCES

(1) Lu, L.; Su, S.; Yang, H.; Jiang, S. Antivirals with common targets against highly pathogenic viruses. *Cell* **2021**, *184*, 2021.

(2) Cui, J.; Li, F.; Shi, Z. L. Origin and evolution of pathogenic coronaviruses. *Nat Rev Microbiol* **2019**, *17*, 181−192.

(3) Bar-On, Y. M.; Flamholz, A.; Phillips, R.; Milo, R. SARS-CoV-2 (COVID-19) by the numbers. *eLife* **2020**, *9*, No. e57309.

(4) Ma, C.; Sacco, M. D.; Hurst, B.; Townsend, J. A.; Hu, Y.; Szeto, T.; Zhang, X.; Tarbet, B.; Marty, M. T.; Chen, Y.; Wang, J. Boceprevir, GC-376, and calpain inhibitors II, XII inhibit SARS-CoV-2 viral replication by targeting the viral main protease. *Cell Res* **2020**, *30*, 678−692.

(5) Sacco, M. D.; Ma, C.; Lagarias, P.; Gao, A.; Townsend, J. A.; Meng, X.; Dube, P.; Zhang, X.; Hu, Y.; Kitamura, N.; Hurst, B.; Tarbet, B.; Marty, M. T.; Kolocouris, A.; Xiang, Y.; Chen, Y.; Wang, J. Structure and inhibition of the SARS-CoV-2 main protease reveal strategy for developing dual inhibitors against M(pro) and cathepsin L. *Sci. Adv.* **2020**, *6*, No. eabe0751.

(6) Ma, C.; Sacco, M. D.; Xia, Z.; Lambrinidis, G.; Townsend, J. A.; Hu, Y.; Meng, X.; Szeto, T.; Ba, M.; Zhang, X.; Gongora, M.; Zhang, F.; Marty, M. T.; Xiang, Y.; Kolocouris, A.; Chen, Y.; Wang, J. Discovery of SARS-CoV-2 Papain-like Protease Inhibitors through a Combination of High-Throughput Screening and a FlipGFP-Based Reporter Assay. *ACS Cent. Sci.* **2021**, *7*, 1245−1260.

(7) Ghosh, A. K.; Brindisi, M.; Shahabi, D.; Chapman, M. E.; Mesecar, A. D. Drug Development and Medicinal Chemistry Efforts toward SARS-Coronavirus and Covid-19 Therapeutics. *ChemMedChem* **2020**, *15*, 907−932.

(8) Xiong, M.; Su, H.; Zhao, W.; Xie, H.; Shao, Q.; Xu, Y. What coronavirus 3C-like protease tells us: From structure, substrate selectivity, to inhibitor design. *Med. Res. Rev.* **2021**, *41*, 41.

(9) Ma, C.; Tan, H.; Choza, J.; Wang, Y.; Wang, J. Validation and invalidation of SARS-CoV-2 main protease inhibitors using the Flip-GFP and Protease-Glo luciferase assays. *Acta. Pharm. Sin. B* **2021**, DOI: 10.1016/j.apsb.2021.10.026.

(10) Ma, C.; Hu, Y.; Townsend, J. A.; Lagarias, P. I.; Marty, M. T.; Kolocouris, A.; Wang, J. Ebselen, Disulfiram, Carmofur, PX-12, Tideglusib, and Shikonin Are Nonspecific Promiscuous SARS-CoV-2 Main Protease Inhibitors. *ACS Pharmacol Transl Sci* **2020**, *3*, 1265−1277.

(11) Gurard-Levin, Z. A.; Liu, C.; Jekle, A.; Jaisinghani, R.; Ren, S.; Vandyck, K.; Jochmans, D.; Leyssen, P.; Neyts, J.; Blatt, L. M.; Beigelman, L.; Symons, J. A.; Raboisson, P.; Scholle, M. D.; Deval, J. Evaluation of SARS-CoV-2 3C-like protease inhibitors using self-assembled monolayer desorption ionization mass spectrometry. *Antiviral Res.* **2020**, *182*, 104924.

(12) Cao, W.; Cho, C.-C. D.; Geng, Z. Z.; Ma, X. R.; Allen, R.; Shaabani, N.; Vatansever, E. C.; Alugubelli, Y. R.; Ma, Y.; Ellenburg, W. H.; Yang, K. S.; Qiao, Y.; Ji, H.; Xu, S.; Liu, W. R. Cellular Activities of SARS-CoV-2 Main Protease Inhibitors Reveal Their Unique Characteristics. *bioRxiv* **2021**, DOI: 10.1101/2021.06.08.447613.

(13) Ma, C.; Wang, J. Dipyridamole, chloroquine, montelukast sodium, candesartan, oxytetracycline, and atazanavir are not SARS-CoV-2 main protease inhibitors. *Proc. Natl. Acad. Sci. U. S. A.* **2021**, *118*, No. e2024420118.

(14) Qiao, J.; Li, Y. S.; Zeng, R.; Liu, F. L.; Luo, R. H.; Huang, C.; Wang, Y. F.; Zhang, J.; Quan, B.; Shen, C.; Mao, X.; Liu, X.; Sun, W.; Yang, W.; Ni, X.; Wang, K.; Xu, L.; Duan, Z. L.; Zou, Q. C.; Zhang, H. L.; Qu, W.; Long, Y. H.; Li, M. H.; Yang, R. C.; Liu, X.; You, J.; Zhou, Y.; Yao, R.; Li, W. P.; Liu, J. M.; Chen, P.; Liu, Y.; Lin, G. F.; Yang, X.; Zou, J.; Li, L.; Hu, Y.; Lu, G. W.; Li, W. M.; Wei, Y. Q.;

Zheng, Y. T.; Lei, J.; Yang, S. SARS-CoV-2 M(pro) inhibitors with antiviral activity in a transgenic mouse model. *Science* **2021**, *371*, 1374−1378.
(15) Dampalla, C. S.; Zheng, J.; Perera, K. D.; Wong, L. R.; Meyerholz, D. K.; Nguyen, H. N.; Kashipathy, M. M.; Battaile, K. P.; Lovell, S.; Kim, Y.; Perlman, S.; Groutas, W. C.; Chang, K. O. Postinfection treatment with a protease inhibitor increases survival of mice with a fatal SARS-CoV-2 infection. *Proc. Natl. Acad. Sci. U. S. A.* **2021**, *118*, No. e2101555118.
(16) Cáceres, C. J.; Cardenas-Garcia, S.; Carnaccini, S.; Seibert, B.; Rajao, D. S.; Wang, J.; Perez, D. R. Efficacy of GC-376 against SARS-CoV-2 virus infection in the K18 hACE2 transgenic mouse model. *Sci. Rep.* **2021**, *11*, 9609.
(17) Boras, B.; Jones, R. M.; Anson, B. J.; Arenson, D.; Aschenbrenner, L.; Bakowski, M. A.; Beutler, N.; Binder, J.; Chen, E.; Eng, H.; Hammond, H.; Hammond, J.; Haupt, R. E.; Hoffman, R.; Kadar, E. P.; Kania, R.; Kimoto, E.; Kirkpatrick, M. G.; Lanyon, L.; Lendy, E. K.; Lillis, J. R.; Logue, J.; Luthra, S. A.; Ma, C.; Mason, S. W.; McGrath, M. E.; Noell, S.; Obach, R. S.; MN, O. B.; O'Connor, R.; Ogilvie, K.; Owen, D.; Pettersson, M.; Reese, M. R.; Rogers, T. F.; Rosales, R.; Rossulek, M. I.; Sathish, J. G.; Shirai, N.; Steppan, C.; Ticehurst, M.; Updyke, L. W.; Weston, S.; Zhu, Y.; White, K. M.; Garcia-Sastre, A.; Wang, J.; Chatterjee, A. K.; Mesecar, A. D.; Frieman, M. B.; Anderson, A. S.; Allerton, C. Preclinical characterization of an intravenous coronavirus 3CL protease inhibitor for the potential treatment of COVID19. *Nat. Commun.* **2021**, *12*, 6055.
(18) Owen, D. R.; Allerton, C. M. N.; Anderson, A. S.; Aschenbrenner, L.; Avery, M.; Berritt, S.; Boras, B.; Cardin, R. D.; Carlo, A.; Coffman, K. J.; Dantonio, A.; Di, L.; Eng, H.; Ferre, R.; Gajiwala, K. S.; Gibson, S. A.; Greasley, S. E.; Hurst, B. L.; Kadar, E. P.; Kalgutkar, A. S.; Lee, J. C.; Lee, J.; Liu, W.; Mason, S. W.; Noell, S.; Novak, J. J.; Obach, R. S.; Ogilvie, K.; Patel, N. C.; Pettersson, M.; Rai, D. K.; Reese, M. R.; Sammons, M. F.; Sathish, J. G.; Singh, R. S. P.; Steppan, C. M.; Stewart, A. E.; Tuttle, J. B.; Updyke, L.; Verhoest, P. R.; Wei, L.; Yang, Q.; Zhu, Y. An oral SARS-CoV-2 M(pro) inhibitor clinical candidate for the treatment of COVID-19. *Science* **2021**, *374*, 1586−1593.
(19) Freitas, B. T.; Durie, I. A.; Murray, J.; Longo, J. E.; Miller, H. C.; Crich, D.; Hogan, R. J.; Tripp, R. A.; Pegan, S. D. Characterization and Noncovalent Inhibition of the Deubiquitinase and deISGylase Activity of SARS-CoV-2 Papain-Like Protease. *ACS Infect Dis* **2020**, *6*, 2099−2109.
(20) Shin, D.; Mukherjee, R.; Grewe, D.; Bojkova, D.; Baek, K.; Bhattacharya, A.; Schulz, L.; Widera, M.; Mehdipour, A. R.; Tascher, G.; Geurink, P. P.; Wilhelm, A.; van der Heden van Noort, G. J.; Ovaa, H.; Müller, S.; Knobeloch, K.-P.; Rajalingam, K.; Schulman, B. A.; Cinatl, J.; Hummer, G.; Ciesek, S.; Dikic, I. Papain-like protease regulates SARS-CoV-2 viral spread and innate immunity. *Nature* **2020**, *587*, 657−662.
(21) Klemm, T.; Ebert, G.; Calleja, D. J.; Allison, C. C.; Richardson, L. W.; Bernardini, J. P.; Lu, B. G.; Kuchel, N. W.; Grohmann, C.; Shibata, Y.; Gan, Z. Y.; Cooney, J. P.; Doerflinger, M.; Au, A. E.; Blackmore, T. R.; van der Heden van, G. J.; Geurink, P. P.; Ovaa, H.; Newman, J.; Riboldi-Tunnicliffe, A.; Czabotar, P. E.; Mitchell, J. P.; Feltham, R.; Lechtenberg, B. C.; Lowes, K. N.; Dewson, G.; Pellegrini, M.; Lessene, G.; Komander, D. Mechanism and inhibition of the papain-like protease, PLpro, of SARS-CoV-2. *EMBO J* **2020**, *39*, No. e106275.
(22) Baez-Santos, Y. M.; St John, S. E.; Mesecar, A. D. The SARS-coronavirus papain-like protease: structure, function and inhibition by designed antiviral compounds. *Antiviral Res.* **2015**, *115*, 21−38.
(23) Shen, Z.; Ratia, K.; Cooper, L.; Kong, D.; Lee, H.; Kwon, Y.; Li, Y.; Alqarni, S.; Huang, F.; Dubrovskyi, O.; Rong, L.; Thatcher, G. R. J.; Xiong, R. Design of SARS-CoV-2 PLpro Inhibitors for COVID-19 Antiviral Therapy Leveraging Binding Cooperativity. *J. Med. Chem.* **2021**, DOI: 10.1021/acs.jmedchem.1c01307.
(24) Shan, H.; Liu, J.; Shen, J.; Dai, J.; Xu, G.; Lu, K.; Han, C.; Wang, Y.; Xu, X.; Tong, Y.; Xiang, H.; Ai, Z.; Zhuang, G.; Hu, J.; Zhang, Z.; Li, Y.; Pan, L.; Tan, L. Development of potent and selective inhibitors targeting the papain-like protease of SARS-CoV-2. *Cell Chem. Biol.* **2021**, *28*, 855−865.e9.
(25) Osipiuk, J.; Azizi, S. A.; Dvorkin, S.; Endres, M.; Jedrzejczak, R.; Jones, K. A.; Kang, S.; Kathayat, R. S.; Kim, Y.; Lisnyak, V. G.; Maki, S. L.; Nicolaescu, V.; Taylor, C. A.; Tesar, C.; Zhang, Y. A.; Zhou, Z.; Randall, G.; Michalska, K.; Snyder, S. A.; Dickinson, B. C.; Joachimiak, A. Structure of papain-like protease from SARS-CoV-2 and its complexes with non-covalent inhibitors. *Nat. Commun.* **2021**, *12*, 743.
(26) Rut, W.; Lv, Z.; Zmudzinski, M.; Patchett, S.; Nayak, D.; Snipas, S. J.; El Oualid, F.; Huang, T. T.; Bekes, M.; Drag, M.; Olsen, S. K. Activity profiling and crystal structures of inhibitor-bound SARS-CoV-2 papain-like protease: A framework for anti-COVID-19 drug design. *Sci. Adv.* **2020**, *6*, No. eabd4596.
(27) Cho, C. C.; Li, S. G.; Lalonde, T. J.; Yang, K. S.; Yu, G.; Qiao, Y.; Xu, S.; Ray Liu, W. Drug Repurposing for the SARS-CoV-2 Papain-Like Protease. *ChemMedChem* **2022**, *17*, No. e202100455.
(28) Lim, C. T.; Tan, K. W.; Wu, M.; Ulferts, R.; Armstrong, L. A.; Ozono, E.; Drury, L. S.; Milligan, J. C.; Zeisner, T. U.; Zeng, J.; Weissmann, F.; Canal, B.; Bineva-Todd, G.; Howell, M.; O'Reilly, N.; Beale, R.; Kulathu, Y.; Labib, K.; Diffley, J. F. X. Identifying SARS-CoV-2 antiviral compounds by screening for small molecule inhibitors of Nsp3 papain-like protease. *Biochem. J.* **2021**, *478*, 2517−2531.
(29) Zhao, Y.; Du, X.; Duan, Y.; Pan, X.; Sun, Y.; You, T.; Han, L.; Jin, Z.; Shang, W.; Yu, J.; Guo, H.; Liu, Q.; Wu, Y.; Peng, C.; Wang, J.; Zhu, C.; Yang, X.; Yang, K.; Lei, Y.; Guddat, L. W.; Xu, W.; Xiao, G.; Sun, L.; Zhang, L.; Rao, Z.; Yang, H. High-throughput screening identifies established drugs as SARS-CoV-2 PLpro inhibitors. *Protein Cell* **2021**, *12*, 877−888.
(30) Swaim, C. D.; Dwivedi, V.; Perng, Y.-C.; Zhao, X.; Canadeo, L. A.; Harastani, H. H.; Darling, T. L.; Boon, A. C. M.; Lenschow, D. J.; Kulkarni, V.; Huibregtse, J. M. 6-Thioguanine blocks SARS-CoV-2 replication by inhibition of PLpro. *iScience* **2021**, *24*, 103213.
(31) Fu, Z.; Huang, B.; Tang, J.; Liu, S.; Liu, M.; Ye, Y.; Liu, Z.; Xiong, Y.; Zhu, W.; Cao, D.; Li, J.; Niu, X.; Zhou, H.; Zhao, Y. J.; Zhang, G.; Huang, H. The complex structure of GRL0617 and SARS-CoV-2 PLpro reveals a hot spot for antiviral drug discovery. *Nat. Commun.* **2021**, *12*, 488.
(32) Pushpakom, S.; Iorio, F.; Eyers, P. A.; Escott, K. J.; Hopper, S.; Wells, A.; Doig, A.; Guilliams, T.; Latimer, J.; McNamee, C.; Norris, A.; Sanseau, P.; Cavalla, D.; Pirmohamed, M. Drug repurposing: progress, challenges and recommendations. *Nat Rev Drug Discov* **2019**, *18*, 41−58.
(33) Mercorelli, B.; Palù, G.; Loregian, A. Drug Repurposing for Viral Infectious Diseases: How Far Are We? *Trends Microbiol.* **2018**, *26*, 865−876.
(34) Park, J. Y.; Kim, J. H.; Kim, Y. M.; Jeong, H. J.; Kim, D. W.; Park, K. H.; Kwon, H. J.; Park, S. J.; Lee, W. S.; Ryu, Y. B. Tanshinones as selective and slow-binding inhibitors for SARS-CoV cysteine proteases. *Bioorg. Med. Chem.* **2012**, *20*, 5928−5935.
(35) Chen, X.; Chou, C. Y.; Chang, G. G. Thiopurine analogue inhibitors of severe acute respiratory syndrome-coronavirus papain-like protease, a deubiquitinating and deISGylating enzyme. *Antiviral Chem. Chemother.* **2009**, *19*, 151−156.
(36) Chou, C. Y.; Chien, C. H.; Han, Y. S.; Prebanda, M. T.; Hsieh, H. P.; Turk, B.; Chang, G. G.; Chen, X. Thiopurine analogues inhibit papain-like protease of severe acute respiratory syndrome coronavirus. *Biochem. Pharmacol.* **2008**, *75*, 1601−1609.
(37) Cheng, K. W.; Cheng, S. C.; Chen, W. Y.; Lin, M. H.; Chuang, S. J.; Cheng, I. H.; Sun, C. Y.; Chou, C. Y. Thiopurine analogs and mycophenolic acid synergistically inhibit the papain-like protease of Middle East respiratory syndrome coronavirus. *Antiviral Res.* **2015**, *115*, 9−16.
(38) Li, W. W.; Heinze, J.; Haehnel, W. Site-specific binding of quinones to proteins through thiol addition and addition-elimination reactions. *J. Am. Chem. Soc.* **2005**, *127*, 6140−6141.
(39) Sargsyan, K.; Lin, C.-C.; Chen, T.; Grauffel, C.; Chen, Y.-P.; Yang, W.-Z.; Yuan, H. S.; Lim, C. Multi-targeting of functional

cysteines in multiple conserved SARS-CoV-2 domains by clinically safe Zn-ejectors. *Chem. Sci.* **2020**, *11*, 9904−9909.
(40) Weglarz-Tomczak, E.; Tomczak, J. M.; Talma, M.; Burda-Grabowska, M.; Giurg, M.; Brul, S. Identification of ebselen and its analogues as potent covalent inhibitors of papain-like protease from SARS-CoV-2. *Sci. Rep.* **2021**, *11*, 3640.
(41) Lin, M. H.; Moses, D. C.; Hsieh, C. H.; Cheng, S. C.; Chen, Y. H.; Sun, C. Y.; Chou, C. Y. Disulfiram can inhibit MERS and SARS coronavirus papain-like proteases via different modes. *Antiviral Res.* **2018**, *150*, 155−163.
(42) Chen, T.; Fei, C. Y.; Chen, Y. P.; Sargsyan, K.; Chang, C. P.; Yuan, H. S.; Lim, C. Synergistic Inhibition of SARS-CoV-2 Replication Using Disulfiram/Ebselen and Remdesivir. *ACS Pharmacol Transl Sci* **2021**, *4*, 898−907.

https://doi.org/10.1021/acsptsci.1c00240
ACS Pharmacol. Transl. Sci. 2022, 5, 102−109